Polarimetric measurements of fabric surfaces

Michel Tourlonias, Laurent Bigue, Marie-Ange Bueno

Michel Tourlonias, Laurent Bigué and Marie-Ange Bueno

Polarimetric measurements of fabric surfaces

Polarimetric measurements of fabric surfaces

Michel Tourlonias
Université de Haute-Alsace
Ecole Nationale Supérieure d'Ingénieurs Sud
    Alsace
Laboratoire de Physique et Mécanique Textiles
    (CNRS UMR 7189)
11, rue Alfred Werner
68093 Mulhouse Cedex, France
    and
Université de Haute-Alsace
Ecole Nationale Supérieure d'Ingénieurs Sud
    Alsace
Laboratoire Modélisation Intelligence Processus
    Systèmes (EA 2332)
12, rue des Frères Lumière
68093 Mulhouse Cedex, France
E-mail: michel.tourlonias@uha.fr

Laurent Bigué, MEMBER SPIE
Université de Haute-Alsace
Ecole Nationale Supérieure d'Ingénieurs Sud
    Alsace
Laboratoire Modélisation Intelligence Processus
    Systèmes (EA 2332)
12, rue des Frères Lumière
68093 Mulhouse Cedex, France

Marie-Ange Bueno
Université de Haute-Alsace
Ecole Nationale Supérieure d'Ingénieurs Sud
    Alsace
Laboratoire de Physique et Mécanique Textiles
    (CNRS UMR 7189)
11, rue Alfred Werner
68093 Mulhouse Cedex, France

Abstract. We describe an optoelectronic setup designed to evaluate the surface parameters of fabrics that influence their tactile feel. The developed texturometer uses the periodic structure of a textile material and its ability to reflect light to evaluate its surface properties through its polarimetric properties. The device scans the surface with a laser line and performs a temporal Fourier analysis of the reflected light, which allows us to consider the periodical structure of the material's surface. Instead of using the overall reflected energy, the analysis is performed on the degree of polarization of light. Results obtained with this new texturometer are compared to those obtained with a nonpolarimetric device that uses overall reflected energy. Emerized and nonemerized twill fabrics are tested, as well as spun-bonded nonwovens. We show that discrimination between samples is enhanced with this polarimetric texturometer. For emerized fabrics, the results exhibit a decrease in depolarization as emerizing intensity increases. For nonwovens, a complementary study in polarimetric imaging has been performed to better understand the phenomena. Nonwoven thermobonded points exhibit lower depolarization of the lightwave than the rest of the structure. Moreover, their depolarization differentiates the tested nonwovens. © *2007 Society of Photo-Optical Instrumentation Engineers.* [DOI: 10.1117/1.2771122]

1 Introduction

One of the most important parameters when a consumer buys a product has proven to be its tactile feel. This notion is essential for a textile material. The authors made several studies in order to understand and evaluate the mechanisms involved in tactile feel.[1,2] This evaluation is usually performed by trained people as a measuring device, but the aim of this study was to perform it in an objective way with physical measurements.

Tactile feel depends on several characteristics: compression, friction, bending, tensile, shear, and thermal behaviors. The subject of this paper is the texture characterization linked to roughness structure and superficial hairiness. In fact, hairiness makes the characterization of fabric texture very specific. Some devices allow the user to determine the profile of the textile surface in order to calculate its roughness parameters. This profile can be determined by laser triangulation methods through a point or a line,[3–5] by studying the light reflection of a laser point,[6,7] by confocal microscopy,[8] or by interferometric methods.[9] For fabrics, these methods are not very efficient in differentiating hairiness from roughness. Other methods use image processing techniques to determine textile surface periodic structure and surface state modifications. These methods use Fourier transform[10–15] or wavelet transform[16–21] to determine periodical structures. Moreover, some filters can be applied to detect defects or pilling. The disadvantage of image processing is due to fabric hairiness. Indeed, in order to detect hairiness, images must present a sufficient resolution. Also, a great number of images is necessary for statistical efficiency, hence, the process takes a long time in terms of image acquisition and processing.

A previous texturometer developed by one of the authors analyzed the total light reflection of a laser line imaged at the surface of the tested sample.[2] During the test, the laser probe described a ring on the fabric since the sample was fixed on a rotating sample carrier, as in a record player. A simple temporal Fourier transform was applied to the acquired signal and allowed the user to determine periodical structure elements. The obtained Fourier spectra, calculated

in real time but time-averaged, presented some peaks whose frequencies corresponded to these periodical structure elements (periods of the yarns or diagonals for a woven fabric or arrangement of the calendering points for spun-bonded nonwovens). It was shown that the surface state influences the energy of these peaks.

The physical phenomena that occurred during this experiment were not deeply studied, but, some surprising results were found. An increase of fabric hairiness could have the opposite effect on reflected light energy depending on the fabric tested. For some fabrics, hairiness decreased the reflected light energy,[2] and for other fabrics, reflected light energy increased with an increases hairiness. These results clearly showed that diffusion, and therefore depolarization, were involved, so it was decided that the depolarizating properties of fabrics should be investigated.

Buck et al. considered the reflection of a light beam at the surface of a fiber and on a plane of parallel fibers.[22] They found that the specular component of fabric depended on its fiber orientation compared to the incidence of the beam. On the other hand, fiber and incident beam orientation have been found to influence the Fresnel coefficients of the fabric surface and the degree of polarization of the reflected beam.[23] However, the reflection on a surface consists of specular[24,25] and diffuse components linked to surface roughness and hairiness. Diffuse components induce phenomena of depolarization of the light wave. To evaluate the influence of both specular and diffuse reflections with textile fabrics, a preliminary study was done.[26] Several authors have also used the degree of polarization of light in order to differentiate materials with the same total reflected light.[27,28] In addition, the degree of polarization has been used for 3-D object reconstruction.[29]

To determine the roughness of surfaces, polarization properties of surface thermal emission also can be considered.[30] The degree of polarization of this emission has been evaluated.[30] It increases with the angle of emission, but this increase is lower when the surface roughness is higher. On the hand, the polarization of the reflected beam on skin allows the influence of skin roughness and physiological properties to be evaluated.[31]

This paper describes a polarimetric texturometer for fibrous materials. The principle is based on a previous texturometer[2] combined with a polarization phenomena measurement. Section 2 describes the tested textile samples and the developed polarimetric devices. Section 3 reports the results obtained with this study.

2 Description of Apparatus and Samples

2.1 Tested Textile Surfaces

Two different kinds of fibrous materials were tested in this study: three types of twill woven fabrics and a spun-bonded nonwoven. In Figs. 1 and 2 and Table 1, the aspect and characteristics of the twill fabric samples through their weave (yarn interlacement) and their dimensional properties are presented. The first (S1) and third (S3) twill woven fabrics, made of cotton fibers, are usually used for pairs of jeans. The second twill fabric (S2), mainly composed of polyester filaments, is used to make women's summer pants.

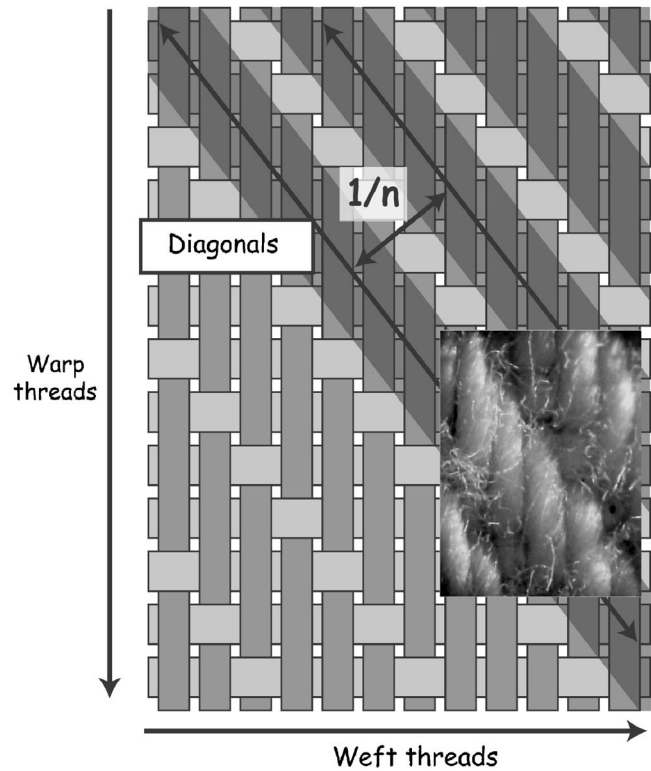To compare different surface states from the same textile

Fig. 1 Presentation of the tested twill fabrics: example of interlacement diagram and interesting structure elements.
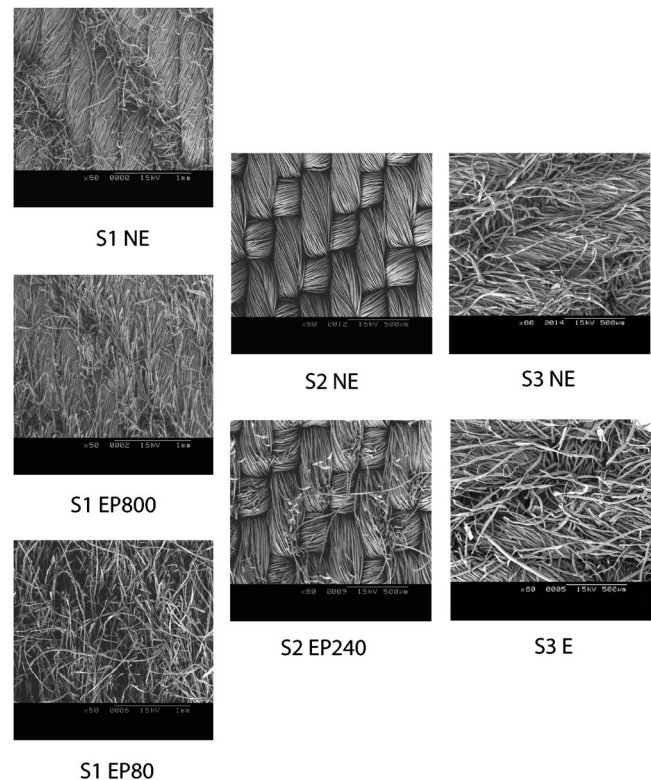

Fig. 2 Photographs of the tested twill fabrics.

Table 1 Structural characteristics of tested twill fabrics.

Notation	Surface State	Material	Number of Elements /cm
S1	NE E-P80 E-P800	100% cotton	28 warp yarns/cm 17 weft yarns/cm 8.5 diagonals/cm
S2	NE E	4% elastane 96% polyester	44 warp yarns/cm 37 weft yarns/cm 21 diagonals/cm
S3	NE E	100% cotton	29 warp yarns/cm 19 weft yarns/cm 11 diagonals/cm

material, the twill samples were emerized. The emerizing process consists of a controlled abrasive wear in which the objective is to improve fabric touch to "peach skin touch," which is a common finishing process. The differences between emerizers S1-EP800 and EP80 are the size and the quantity of the abrasive particles of their emery paper. The P800 emery had 800 grains per mm^2 with a 21.8-μm mean diameter. The second sample was emerized using a P80 paper with about 80 particles per mm^2, whose size was 201-μm mean diameter. The process with the P80 emery was more aggressive than with the P800 emery. An emerized form of the second twill fabric was also used. It was made with a paper constituted of about 240 grains per mm^2 whose diameter was 58.5 μm. Both were laboratory emerized to precisely control the process. The emerized form of the third sample was industrially obtained, so the process adjustments for this emerized fabric were not known.

A spun-bonded nonwoven for medical use was also studied. Two samples were available; one was defined by the manufacturers as "not in conformity" in terms of softness compared to the second one (Fig. 3). The cohesion of this filament web was obtained by thermobonding.

In conformity   Not in conformity

d1 = d2 = 4.5 points / cm
Peak 1

D1 = D2 = 5.5 points / cm
Peak 2

Thermobonding point
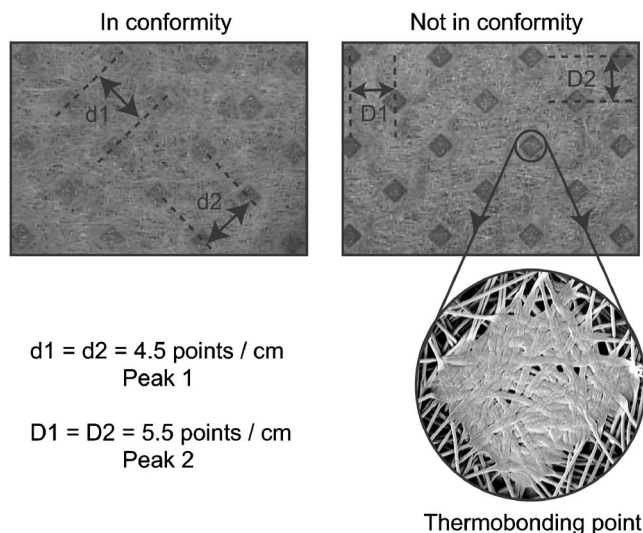
Fig. 3 Diagram of the spun-bonded nonwovens.

2.2 Polarization Basis and Notations

A lightwave is defined as an electromagnetic wave whose polarimetric characteristics can be completely represented by its Stokes vector:

$$\vec{S} = \begin{bmatrix} S_0 \\ S_1 \\ S_2 \\ S_3 \end{bmatrix} = \begin{bmatrix} I_p + I_s \\ I_p - I_s \\ I_{+45} - I_{-45} \\ I_r - I_l \end{bmatrix}, \tag{1}$$

where

I_p is the linearly polarized component along horizontal axis,

I_s is the linearly polarized component along vertical axis,

I_{+45} is the linearly polarized component at 45°,

I_{-45} is the linearly polarized component at −45°,

I_r is the right circularly polarized component,

and

I_l is the left circularly polarized component.

The degree of polarization of such a light beam is defined as

$$P = \frac{I_{\text{pol}}}{I_{\text{tot}}} = \frac{\sqrt{S_1^2 + S_2^2 + S_3^2}}{S_0}, \tag{2}$$

where S_0 corresponds to the total light intensity of the lightwave, and the other components correspond to the polarized parts:

When $P=1$, the wave is totally polarized.
When $P=0$, the wave is totally nonpolarized.
If $0 < P < 1$, P represents the amount of beam polarization.

2.3 Preliminary Imaging Setup

A first imaging assembly was made to calculate the Stokes vector of the wave reflected by each fabric sample. The sample was illuminated by a linearly polarized laser beam, and the Stokes parameters were evaluated by rotating a polarizer and/or quarter-wave plate. But the problem of parallelism between the two sides of the polarizer plate caused a shift between pixels of images obtained by rotation of this polarizer. Therefore, the measurement principle of Terrier was used.[32] From image acquisitions by the optical device shown in Fig. 4 with different angular positions of the quarter-wave plate L3, the Stokes parameters of the light wave reflected by the sample were determined according to
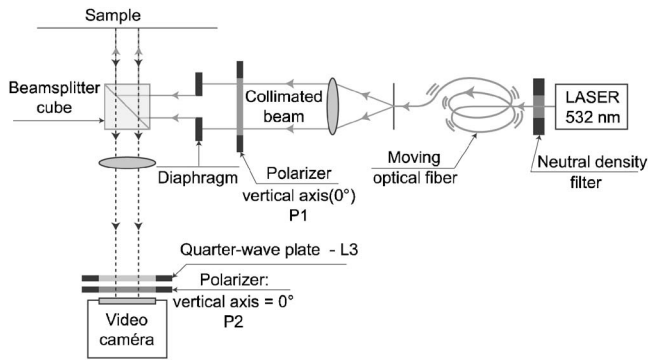
Fig. 4 Diagram of the optical system used for the polarimetric imaging study.

Fig. 5 Diagram of the optical system of the polarimetric texturometer.

$$I(\theta) = \frac{1}{2}[S_0 + S_1 \cos^2 2\theta + S_2 \sin 2\theta \cos 2\theta - S_3 \sin 2\theta], \quad (3)$$

where θ is the angular position of L3 relative to the incident polarization,

S_i are components of the Stokes vector of the beam,

and

I is the light intensity of the beam.

This preliminary system for polarimetric imaging allowed us to evaluate the polarization properties of the reflected laser beam at the sample surface. In this study, with our textile samples in normal incidence, we showed with a linearly polarized beam that only phenomena of depolarization occurred, i.e., only the first two elements of the Stokes vector were nonzero. Thus, it was possible to realize a simplification common in optics by assuming that since $S_2 \approx S_3 \approx 0$ (no rotation and no circularization of the polarization occur), the degree of polarization of the wave from the components I_p and I_{90} could be calculated. In this case, the incident probe was polarized along the horizontal axis; I_p, relative to the horizontal polarization, was renamed $I_\parallel$, and I_s was then I_{cross}. Thus, the Stokes vector can be expressed as

$$\vec{S} = \begin{bmatrix} S_0 \\ S_1 \\ S_2 \\ S_3 \end{bmatrix} = \begin{bmatrix} I_p + I_s \\ I_p - I_s \\ I_{+45} - I_{-45} \\ I_r - I_l \end{bmatrix} = \begin{bmatrix} I_\parallel + I_{cross} \\ I_\parallel - I_{cross} \\ 0 \\ 0 \end{bmatrix}, \quad (4)$$

and the degree of polarization comes down to

$$P = \frac{I_{pol}}{I_{tot}} = \frac{\sqrt{S_1^2}}{S_0} = \frac{|S_1|}{S_0} = \frac{|I_\parallel - I_{cross}|}{I_\parallel + I_{cross}}. \quad (5)$$

Therefore, in this case, the polarization of the reflected beam is totally defined by the two crossed linear polarization components $I_\parallel$ and I_{cross}. It is sufficient to register both signals in order to totally characterize the lightwave.
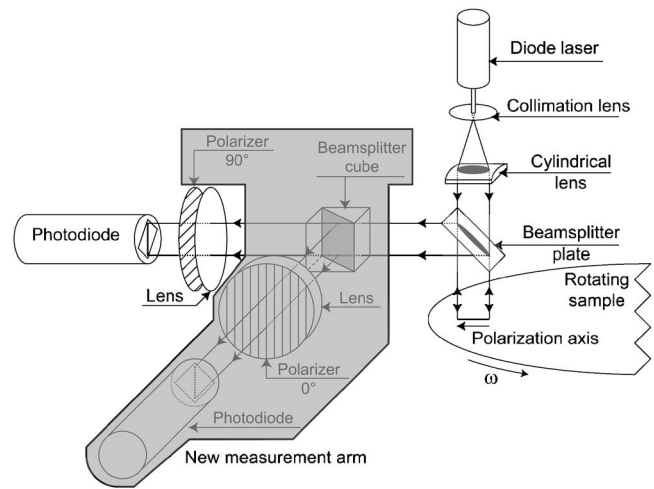
2.4 Polarimetric Texturometer

Out optical device used the measurement principle (Fig. 5) presented by Bueno et al.[2] The sample was clamped on a rotating sample carrier as in a record player. A laser beam projected by a 650-nm laser diode onto the sample was focused as a line at the surface by passing through a cylindrical lens. The laser line was radial to the rotating sample carrier. A beamsplitter plate sent the reflected beam to the photodiode. The length of the laser line was adjusted to $8 . 10^{-3}$ m. Several sample carriers were available to test textile fabrics whose sizes varied from 10 to $20 . 10^{-2}$ m diameter. The laser line was focused and aligned with the center of the rotation of the sample carrier in order to be radial, so during the rotation of the sample carrier, it scanned the textile surface following a ring.

For the tests presented in this paper, the diameter of the ring was about $10 . 10^{-2}$ m and the rotation speed was adjusted to 0.25 rps. In this original device, the total reflected beam was concentrated onto a photodiode.

In order to simultaneously acquire $I_\parallel$ and I_{cross}, which was sufficient in our case to define the degree of polarization of the reflected beam, a second measurement arm was added to the optical device. A beamsplitter cube separated the lightwave reflected by the sample into the two measurement arms. On the optical path of the first arm, a polarizer was inserted whose main direction was parallel to the polarization direction of the incident beam, i.e., parallel to the laser line. In the same way, a polarizer crossed to this direction was inserted in the optical path of the second arm. The two signals were acquired simultaneously, and the degree of polarization was hardware calculated from these components according to Eq. (5).

The variations of light intensity during measurement depended on the structure of the textile surface. For example, in the case of the twill woven structure, while the laser line described the ring, it was sometimes parallel or quasi-parallel to the diagonals described by the yarn interlacements. Intensity variations of the beam received by the photodiode corresponded to this alteration. The frequency of these phenomena can be evaluated with an appropriate
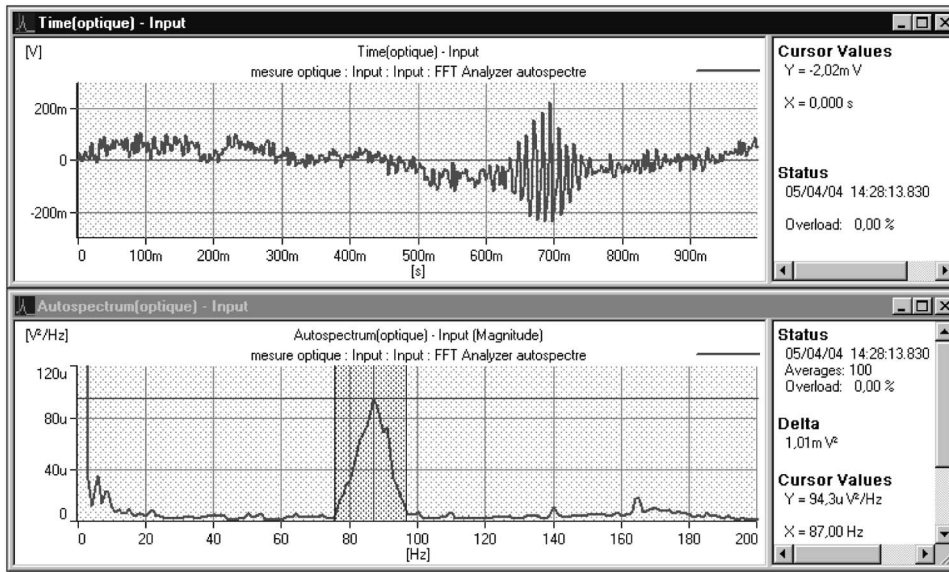
Fig. 6 Example of the temporal intensity signal received by the photodiode in the top plot, and its associated Fourier transform in the bottom plot.

signal-processing technique as shown in Fig. 6. This signal-processing technique uses the periodicity of the textile surface; it can be a structural periodicity (fabric) or the result of thermobonding patterns (nonwovens). When the linearly polarized laser line describes and lights the surface, the linearly polarized reflected light components acquired by the two photodiodes change. The received signal in each arm is directly linked to the intensity variation of the reflected beam for both polarization directions, parallel and crossed to the incident polarization. The corresponding signals are sent to a spectral analyzer, which calculates in real time the associated degree of polarization. The Fourier transform of this type of signal is

$$X(f) = \sum_{k=-\infty}^{k=+\infty} x(k) \exp(-j \times 2\pi f k), \qquad (6)$$

where $x(k)$ is the temporal signal,
and
$X(f)$ is the Fourier transform of the signal
$x(k)$.

This study considers the power spectral density (PSD) of the signal:

$$\mathrm{PSD}(f) = |X(f)|^2. \qquad (7)$$

The graphs we obtained exhibit peaks whose frequencies correspond to the periodical structure patterns of the samples (Fig. 7). But the energies of these peaks strongly depend on the surface state.

The theoretical formulas that give the structure frequencies are:

$$P = \pi\phi, \qquad (8)$$

where P is the average perimeter of rotation
(10^{-3} m), and

ϕ is the average ring diameter measured in the middle of the laser line (10^{-3} m);

$$V = Pf_r, \qquad (9)$$

where V is the linear speed of the laser beam
(10^{-3} m·s^{-1}), and
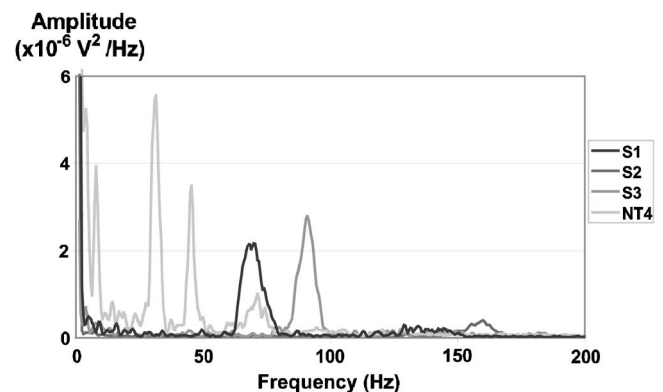
f_r is the rotation speed of the laser line (rps); and

Fig. 7 Example of spectra obtained with our tested fabric.

$$F = Vn, \tag{10}$$

where F is the frequency of the element (Hz), and n is the number of structure elements by unit of length (10^{-3} m^{-1}).

Therefore,

$$F = \pi \phi f_r n. \tag{11}$$

It is also possible to determine the peak width compared with the laser line length:

$$\Delta F = \pi f_r n (\phi_{\max} - \phi_{\min}). \tag{12}$$

For instance, for a twill woven fabric, the interlacement of warp and weft yarns define diagonals (Table 1). Diagonals give the structure frequency in the Fourier spectrum (Fig. 1). With the spun-bonded nonwoven, the frequencies are defined by the distances between the thermobonding points in the two main directions. This pattern and its parameters are shown in Fig. 3.

In the polarimetric texturometer, the degree of polarization is treated as an input signal: actually, signal from both arms are acquired simultaneously and the analyzer performs analysis on the resulting degree of polarization. Through the Fourier transform, this measurement principle takes the periodical structure and the hairiness of the surface into account.

3 Results and Discussion

3.1 Results

Results for twill woven fabrics are presented in Fig. 8, from both nonpolarimetric and polarimetric texturometers. The bar charts represent the energy of the diagonal peak of the autospectra for fabrics before and after the emerizing process. It is interesting to note that all results obtained with emerized samples present the lowest energy for the measurement done with the polarimetric texturometer. Therefore, the effect of hairiness is the same by considering the degree of polarization. In contrast, with the nonpolarimetric texturometer the peak energy increases with the emerizing intensity for the twill woven fabric S1, and decreases for S2 and S3.

We can also note that the discrimination is better by considering the degree of polarization. In fact, the ratio between the energies of the peaks obtained for the same sample with different surface states is higher, as specified in Figs. 8 and 9. For instance, ratios obtained with S1 go between the nonemerized form and P800 emerizing from 1.32 to 2.50, and between P800 and P80 emerizing from 1.24 to 2.04. Results obtained by testing nonwovens with the polarimetric texturometer also present a better discrimination between "in conformity" and "not in conformity" samples (Fig. 9). Nevertheless, energy is higher for both structure peaks for the "not in conformity" nonwoven using the nonpolarimetric device, contrary to results obtained with the polarimetric texturometer, which do not present the same tendency for peak 1 and peak 2.

Because of these differences, a complementary polarimetric imaging study was done on nonwovens.[26] It showed that the degree of polarization of the beam reflected by the
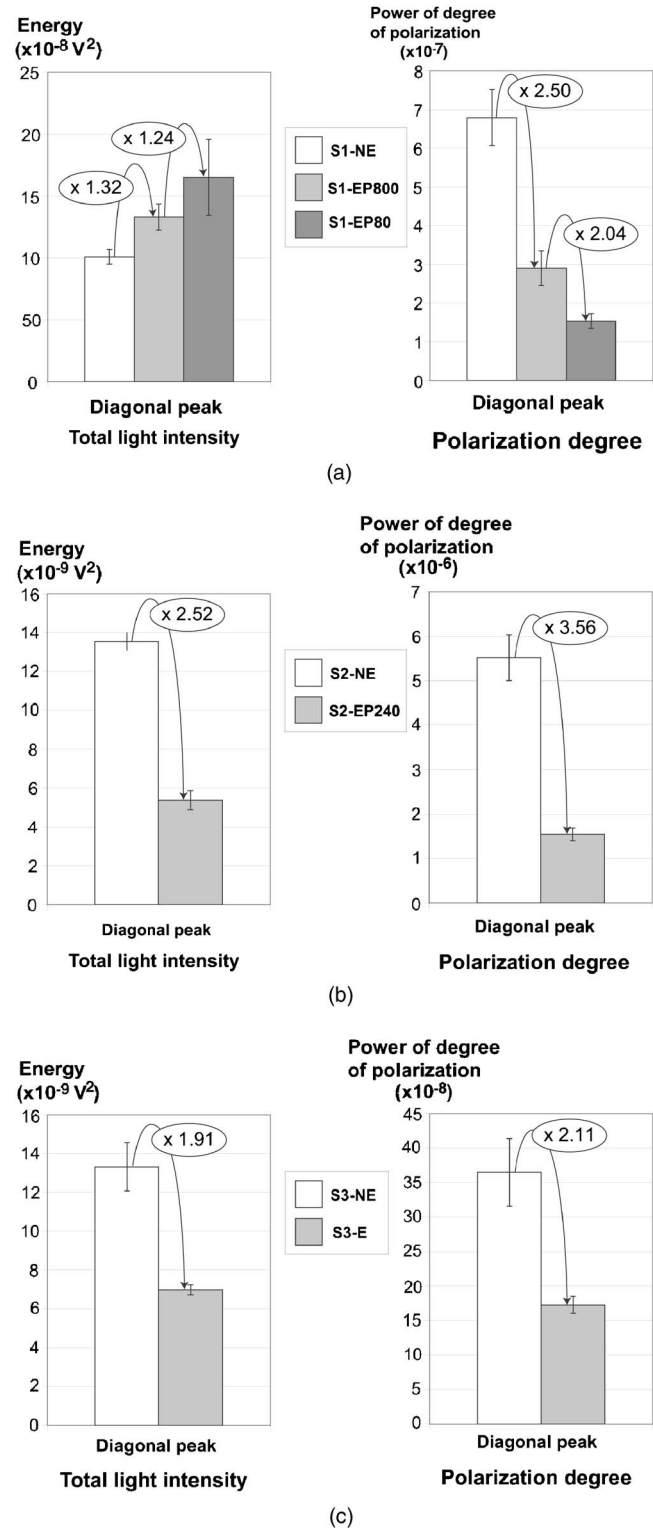

Fig. 8 Bar charts of energy peaks obtained from twill fabric samples with ratio values in (a) S1, (b) S2, and (c) S3.

sample was higher for the bonded point than the other areas of the surface. This trend was also confirmed by considering the sum column gray levels of a basic stripe (Fig. 10). It shows that the discrimination between both nonwoven
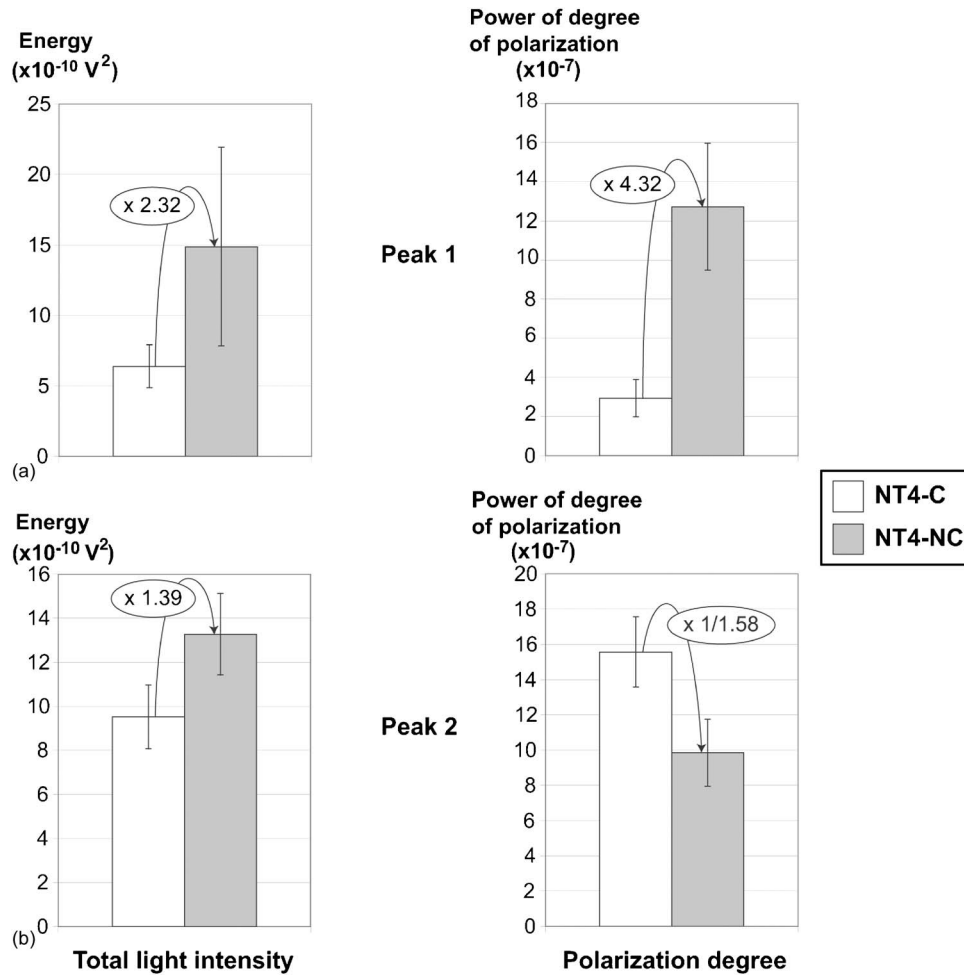
Fig. 9 Bar charts of energy peaks obtained from nonwoven samples with ratio values for (a) the first structural peak, and (b) the second structural peak.

samples in terms of softness conformity comes from bonded points: the depolarization is lower for the bonded points.

As shown by the standard deviation of the measure in Figs. 8 and 9, repeat tests of the nonpolarimetric and polarimetric methods are quite similar.

3.2 Discussion

Results obtained for twill woven fabrics with the polarimetric texturometer allow a better discrimination up to a 1:1.89 ratio and prove that hairiness has increased depolarization at the surface of the samples. This phenomenon is due to random fiber orientation induced at the surface. When the diffuse component increases, the consequence is a decrease of the frequency peak energy since the emerizing intensity increases. With the nonpolarimetric device, for the different twill woven fabrics the emerizing the intensity does not always have the same effect on the structure peak energy. In fact, this device evaluates the diagonal profile, i.e., height and hairiness variations. The profile changes after the emerizing process according to the emery paper used and the fabric's characteristics. The peak energy can evolve with the emerizing intensity relative to the fabrics.

The study of the nonwovens allows a better discrimination up to a 1:1.86 ratio between samples, with measures performed on the degree of polarization of the reflected beam (Fig. 9). In fact, the degree of polarization highlights the differences between bonded points and the other areas of the surface. The polarimetric imaging study, and particularly the mean of the gray level in each column of a basic stripe, allow us to understand this phenomenon. With the polarimetric device, the inversion of the energy classification between both of the nonwoven structure peaks can be explained by the orientation of polarization of the incident beam compared to the main fiber orientation and structure direction (Fig. 10). In the present configuration, the polarization axis of the incident beam is parallel to the laser line. For peak 1, at each quarter-turn the laser line makes an angle of 45 deg relative to the main fibrous direction (Fig. 11). And at each quarter-turn, the laser line is aligned with the structure element of peak 2. Therefore, sometimes the laser line, and thus the polarization axis, is parallel to the main fibrous direction, and sometimes it is perpendicular. We suppose that for peak 1, the energy is the same for each quarter-turn of the sample, but with peak 2, the energy is not equal because the polarimetric axis changes relative to
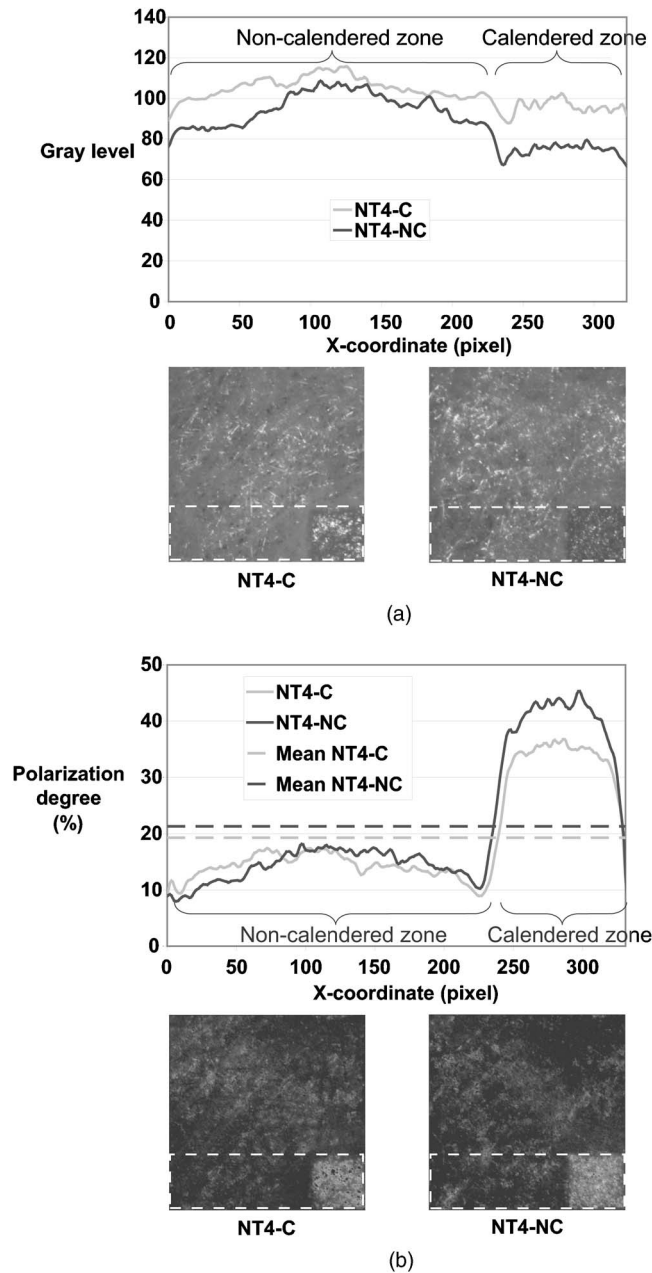
(a)

(b)

Fig. 10 Results obtained with polarimetric imagery of a nonwoven fabric. The curves are plotted by average gray levels of images along the vertical direction in each rectangle with dotted lines on the image in (a) total intensity, and (b) in the polarization degree.

the main fibre orientation. These results show that it is possible to obtain information about the filament orientation in the structure.

This study shows the polarimetric properties of the nonwovens, particularly of the bonded points. Differences between the samples are due to a problem in the calendering process through higher temperature or pressure. In fact, the more intensive the calendering process is, the more reflective are the spun-bonded points.

4 Conclusion

This paper shows that a modification of the surface state of fabrics, woven or nonwoven, can be characterized by tak-
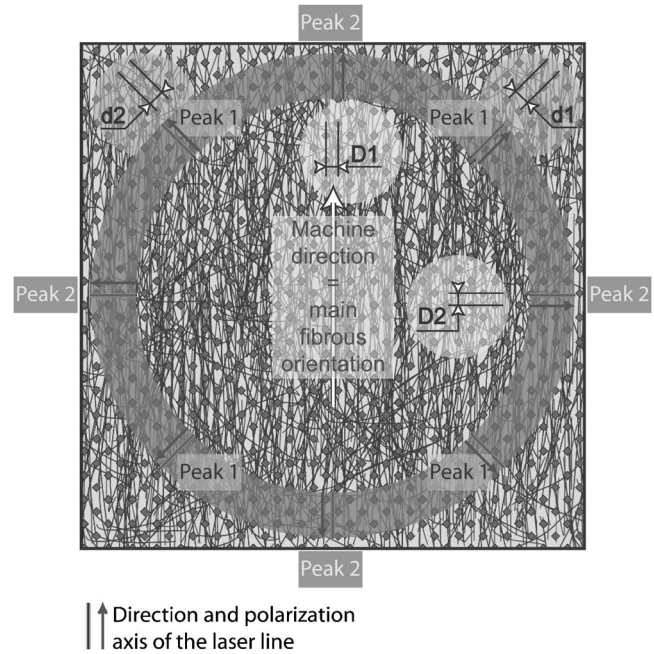

Fig. 11 Polarization of an incident beam in the polarimetric texturometer and the main fibrous orientation.

ing polarimetric properties of these surfaces into account. However, the degree of polarization is a pertinent characteristic of both fabric roughness and hairiness, and of thermobonding in nonwovens.

The principle of the measurement method presented consists in projecting a laser beam onto the fabric surface and studying the degree of polarization of the reflected beam. This signal is then processed with Fourier analysis. The PSD presents several frequency peaks due to fabric periodic structure. The energy of these peaks depends on the fabric surface state.

Two kinds of fabrics have been tested: woven fabrics processed with different emerizing intensities, and nonwovens considered to be in conformity or not in conformity in terms of softness.

The depolarization of the reflected beam is enhanced with fabric hairiness. Therefore, it is easier to discriminate the same fibrous material with different surface states. Moreover, by considering polarization phenomena, hairiness decreases the degree of polarization measured by the polarimetric texturometer presented in this paper. In fact, hairiness increases depolarization due to surface disorder. For thermobonded nonwovens, the control process in terms of softness has also been improved by the polarimetric texturometer. In addition, the polarimetric imaging study allows us to understand that the difference between these nonwovens comes from the thermobonded areas, i.e., from the calendering process, probably due to changes in temperature and/or pressure conditions. However, from some results obtained with nonwovens, we might obtain information about the filament orientation in the structure.

References

1. M.-A. Bueno, B. Durand, and M. Renner, "Noncontact measurements of sandingand raising effects," *Text. Res. J.* **69**(8), 570–575 (1999).
2. M.-A. Bueno, B. Durand, and M. Renner, "Optical characterization of the state of fabric surfaces," *Opt. Eng.* **39**(6), 1697–1703 (2000).
3. R.-B. Ramgulam, J. Amirbayat, and I. Porat, "Measurement of fabric roughness by a non-contact method," *J. Text. Inst.* **84**(1), 99–106 (1993).
4. R. Seifert, P. Raue, P. Offermann, T. Bahners, E. Schollmeyer, M. Mägel, and H. Fuchs, "Surface characterisation of textile fabrics. part 3: profilometric measuring systems," *Melliand Textilberichte/ International Textile Reports* **76**(9), 636–639/E164-E166 (1995).
5. T. Bahners, E. Schollmeyer, R. Seifert, P. Raue, P. Offermann, M. Mägel, and H. Fuchs, "Surface characterisation of textile fabrics. part 4: characterizing the effect of mechanical surface treatments," *Melliand Textilberichte/International Textile Reports* **76**(10), 833–838/ E210-E212 (1995).
6. H. Ishizawa, T. Nishimatsu, M. Kamijyo, and E. Toba, "Measurement of surface properties of woven fabrics using an optical bundle," *J. Textile Engineering* **48**(1), 5–10 (2002).
7. W. Ringens, T. Bahners, and E. Schollmeyer, "Characterisation and control of thread datain textile processes using optical profilometry," *Melliand Textilberichte/International Textile Reports* **83**(20), 715–716/E140 (2002).
8. J.-M. Becker, S. Grousson, and M. Jourlin, "Surface state analysis by means of confocal microscopy," *Cem. Concr. Compos.* **23**(2-3), 255–259 (2001).
9. M. Conte, Y. Jamet, J. Duhamel, M. Jarrigeon, and M. Calonnier, "Roughness measurement by laser," *Industrie Textile* (1212), 105–107 (1990).
10. D.-M. Tsai and C.-Y. Hsieh, "Automated surface inspection for directional textures," *Image Vis. Comput.* **18**(1), 49–62 (1999).
11. E.-J. Wood, "Applying Fourier and associated transforms to pattern characterization in textiles," *Text. Res. J.* **60**(4), 212–220 (1990).
12. E.-J. Wood, "Objective measurement of carpet appearance by image analysis, part 1: principles and methodology", *Melliand Textilberichte/International Textile Reports* **77**(7-8), 452–459/E99-E102 (1996).
13. M. S. Millan and J. Escofet, "Fourier-domain-based angular correlation for quasiperiodic pattern recognition. Applications to web inspection," *Appl. Opt.* **35**(31), 6253–6260 (1996).
14. B. Xu, "Identifying fabric structures with fast fourier transform techniques," *Text. Res. J.* **66**(8), 496–506 (1996).
15. J. Haggerty and M. Young, "Spatial light modulator for texture classification," *Appl. Opt.* **28**(23), 4992–4995 (1989).
16. A. Latif-Amet, A. Ertuzun, and A. Ercil, "An efficient method for texture defect detection: sub-band domain co-occurrence matrices," *Image Vis. Comput.* **18**(6-7), 543–553 (2000).
17. M. Kreißl, S. Heiko, and S. Teiwes, "Optical processor for real-time detection of defects in textile webs," *Proc. SPIE* **3073**, 307–311 (1997).
18. J. Escofet, R. Navarro, M. S. Millan, and J. Pladellorens, "Detection of local defects in textile webs using Gabor filters," *Opt. Eng.* **37**(8), 2297–2307 (1998).
19. D.-M. Tsai and B. Hsiao, "Automatic surface inspection using wavelet reconstruction," *Pattern Recogn.* **34**(6), 1285–1305 (2001).
20. D.-M. Tsai and C.-H. Chiang, "Automatic band selection for wavelet reconstruction in the application of defect detection," *Image Vis. Comput.* **21**(5), 413–431 (2003).
21. C. Shakher, S.-M. Istiaque, and S.-K. Singh, "Application of wavelettransform in characterization of fabric texture," *Proc. SPIE* **4929**, 158–164 (2002).
22. G. S. Buck and F. A. McCord, "Luster and cotton," *Text. Res. J.* **19**(11), 715–755 (1949).
23. D. Goldstein, *Polarized Light*, Second Edition, revised and expanded. Marcel Dekker, New York, Basel (2003).
24. S. K. Nayar, K. Ikeuchi, and T. Kanade, Surface reflection: Physical and geometrical perspectives," Technical Report CMU-RI-TR-89-07, Robotics Institute, Carnegie Mellon University, 1989, pp. 1–59.
25. S. K. Nayar, K. Ikeuchi, and T. Kanade, "Surface reflection: physical and geometrical perspectives," *IEEE Trans. Pattern Anal. Mach. Intell.* **13**(7), 24 (1991).
26. M. Tourlonias, "Caractérisation optique de surfaces textiles: Aspects dynamiques et polarimétriques," Thesis, Université de Mulhouse (France), 2005, pp. 1–117.
27. S. Breugnot and P. Clémenceau, "Modeling and performances of a polarization active imager at $\lambda = 806$ nm," *Proc. SPIE* **3707**, 449–460 (1999).
28. S. Breugnot, "SAMBA: Systeme de vision polarimetrique pour la mesure de l'apparence visuelle: couleur, brillance, texture et defauts de surface," *Journée Imagerie Polarimétrique GDR ISIS*, Paris (2004).
29. O. Morel, C. Stolz, F. Meriaudeau, and P. Gorria, "Active lighting applied to three-dimensional reconstruction of specular metallic surfaces by polarization imaging," *Appl. Opt.* **45**, 4062–4068 (2006).
30. A. C. Dogariu and G. D. Boreman, "Rough-surface polarization effects of infrared emission," *Proc. SPIE* **2828**, 162–170 (1996).
31. B. Boulbry, T.-A. Germer, and C. Ramella-Roman, "A novel hemispherical spectro-polarimetric scattering instrument for skin lesion imaging," *Proc. SPIE* **6078**, 60780R (2006).
32. P. Terrier and V. Devlaminck, "Système polarimétrique pour l'analyse d'images," *Trait. Signal* **17**(5-6), 479–490 (2000).

Michel Tourlonias obtaining his textile engineer diploma at the College of Textiles of Mulhouse (France), then received his PhD degree at the University of Mulhouse in 2005. Since 2005, he has been a post-doctorate at the University of Mulhouse, Ecole Nationale Supérieure d'Ingénieurs Sud Alsace (ENSISA). He is a member of the Société Francaise d'Optique (SFO) and European Optical Society.

Laurent Bigué received his engineering degree at the ENSPS (French College of Physics, Strasbourg, France) as well as his post-graduate degree in photonics and microelectronics at the Université Louis Pasteur, Strasbourg, in 1992. He obtained a PhD in optical, electrical, and computer engineering at the Université de Haute Alsace in 1996. He was appointed as assistant professor at ENSISA (College of Engineering of Université de Haute Alsace, Mulhouse, France) in 1998 and has been a professor at ENSISA since 2005. His major interests include optical signal processing, polarimetry, and optical metrology. He is a member of Société Francaise d'Optique (SFO), SPIE, and EOS.

Marie-Ange Bueno obtained her textile diploma, then received her PhD degree at the University of Mulhouse (France) in 1995. Since 1997, she has been an assistant professor in textile and mechanical engineering, and since 2005 a full professor at the College of Textiles of Mulhouse, Ecole Nationale Supérieure d'Ingénieurs Sud Alsace (ENSISA). She has worked since 1992 on optical or mechanical characterization of fibrous material surface. She is a member of Société Francaise d'Optique (SFO), EOS, and the Fiber Society.